ISSN 2176-5480

22nd International Congress of Mechanical Engineering (COBEM 2013)
November 3-7, 2013, Ribeirão Preto, SP, Brazil

NUMERICAL ANALYSIS OF FLUID SEALS APPLIED TO ROTATING MACHINERY

Larissa Galera
Katia Lucchesi Cavalca
Laboratory of Rotating Machinery – Faculty of Mechanical Engineering – Postal Box 6122
University of Campinas – UNICAMP
13083-970, Campinas, SP, Brazil
lgalera@fem.unicamp.br; katia@fem.unicamp.br

Abstract. *The rotating machinery are essential for many applications. Some rotating components play an important role in the rotating system response and, consequently, influence the analysis of the system. Therefore, the study of rotating machinery components is very important once this analysis, through the mathematical development, intends to predict the dynamic behavior responses of the machine, providing essential information to avoid unexpected problems or failures. Therefore, the dynamic study is not only restricted to the analysis of the behavior of the rotor, but it is also necessary to considerate the interaction between the components involved in their construction, for example bearings, fluid seals, rotors, shafts and supporting structures. The fluid seals cause reaction-forces, which can be represented for dynamic coefficients, such as the direct and cross-coupled stiffness, the direct and cross-coupled damping and inertia. This component is mainly responsible for the differences between a model using only a rotor-bearing and the actual vibration of the set, for example in centrifugal pumps. Therefore, the fluid seals must be mathematically studied in order to add their dynamic coefficients to the global model of rotating systems to make the analysis of the rotating set more complete. In this work, these coefficients are determined for a straight plain fluid seal. The difference between the pressure in the inlet and the outlet of mechanical seals (pressure drop) is obtained through the governmental equations for liquids, such as continuity equation, axial and circumferential momentum equations, using in this case the finite volume method. The equivalent stiffness, damping and inertia coefficients are estimated, and besides, the influence of various physical parameters on the behavior of plain fluid seals is analyzed. The results are initially validated through direct comparison with the values presented in the literature*

Keywords: *plain seals, finite volume method, rotating machinery, dynamic coefficients.*

1. INTRODUCTION

The gaskets are used in the industrial sector for many applications, such as in the automobile, aircraft and space industries, energy generation and pumps production, since their functions are to isolate places with different pressures, temperatures or fluids. Besides, they also prevent the entrance of strange elements in the system. The specific type of gasket for rotating machinery is known as fluid, or mechanical, seal.

The fluid seals are essential for medium and large rotating machinery. Their main objective is to control the leakage of working and lubricating fluids through the interface between rotor and stator. Because of that, they cause a significant influence on the dynamics of rotating systems due to the pressure drop between their inlet and outlet.

The fluid seals can be classified in many different groups. According to Vance (1988), the major classification divided the rotating seals in: plain seals, floating ring oil seals, labyrinth seals and contact seals.

Plain seals are usually used in pumps and they can be straight, tapered or stepped. Their geometry is similar to journal bearing but the ratio between the clearance and the radius of the shaft is commonly twice to ten times larger to avoid contact between rotor and stator.

The analysis of fluid seals is related to the study of rotating machinery, especially to the development of lubrication theory, which is applied in bearings. From this equation, the knowledge was expanded for mechanical seals.

Reynolds (1886) developed an equation to explain experimental measurements about the sustention of the rotor by an oil film. This equation provides the pressure distribution in bearings and it is the basis of modern lubrication theory. However the Reynolds' equation cannot be applied in fluid seals because this component has a turbulent behavior, which can cause considerable errors seeing that bearings are considered to work in laminar flow.

Lomakin (1958) analyzed the causes and consequences of the reaction-forces in mechanical seals, which act in opposite direction of the shaft displacement. In this work, Lomakin obtained the direct-stiffness due to pressure gradient between the inlet and the outlet of mechanical seals. Thus, the combined effect of the inlet loss and the axial pressure gradient is known as "Lomakin effect", which explain the large direct stiffness in plain seals.

Childs (1993) determined the dynamic coefficients for a straight seal using the perturbation method to solve the "Bulk-flow" versions of Navier-Stokes equations. Besides, he also analyzed the influence of various physical parameters on the coefficients behavior.

ISSN 2176-5480

Kwanka (2000) reported that the destabilizing forces are caused by the cross-couple stiffness terms, which are counterbalanced by the terms of direct damping. Thus, the study of damping terms is very important on the analysis of fluid seals.

Moreover, he verified that the conservative coefficients, which are represented by the direct stiffness and cross-coupled damping, influence the vibration frequency of the system, while the non-conservative coefficients, which are the cross-coupled stiffness and direct damping, change the stability limit of the system.

Recently Shen et al. (2008) simulated a model using rotor-bearing-foundation-labyrinth seal, for that, they used the finite element method. The theoretical results and experimental data were compared and the model was validated.

Thereby, this work aims to determine the dynamic coefficients for a nominal straight seals and then compare the results with literature. It will also verify the behavior of these components with respect to various physical and operational parameters, such as rotational speed, pressure gradient and ratio of the seal length and diameter of the shaft.

2. METHODOLOGY

Stiffness, damping and inertia coefficients are evaluated from the reaction-forces in mechanical seals, which are obtained through integration of pressure distribution along the seal. These forces can be linearized for small displacements of the shaft around the equilibrium position and they can be represented as shown in Eq. (1).

$$\begin{Bmatrix} \quad \\ \quad \end{Bmatrix} = [\ \ ]\begin{Bmatrix} \ddot{\ } \\ \ddot{\ } \end{Bmatrix} + \begin{bmatrix} \quad \end{bmatrix}\begin{Bmatrix} \dot{\ } \\ \dot{\ } \end{Bmatrix} + \begin{bmatrix} \quad \end{bmatrix}\begin{Bmatrix} \quad \\ \quad \end{Bmatrix} \tag{1}$$

Where M is the inertia coefficient, K and C are, respectively, the direct stiffness and damping, k and c, in this order, are the cross-coupled stiffness and damping, F_x and F_y are the reaction-forces where x and y are the rectangular coordinates, which also represent the displacement of the shaft in these directions. The "dot" indicates time derivate, thus ˙ and ˙ are the velocities and ¨ and ¨ represent the acceleration of the shaft.

To determine the pressure distribution along the seal, the continuity, axial-momentum and circumferential-momentum equations, which are derived through a basic equation, presented by Fox and McDonald (2006), must be solved for a centered seal and, after that, for a small displacement of the shaft, which makes possible to obtain the reaction-forces.

Equations (2), (3) and (4) represent, respectively, the continuity equation, the axial-momentum and the circumferential-momentum equations.

$$\quad \tag{2}$$

$$\quad \tau_Z^r \ \tau_Z^s \quad \left(\quad \right) \tag{3}$$

$$\quad \left(\quad \right) \tag{4}$$

Where τ is the shear stress, which is calculated using Moody wall-friction model, the superscripts r and s represent, in this order, the rotor and stator wall where τ acts, Z and are the polar coordinates, H is the clearance function, which depends on each type of seal, R is the radius of the shaft, U and W are, respectively, the circumferential and axial velocity components, t represents the time, is density and P is the pressure.

The clearance function (H) changes its value for each type of plain seal. Equation (5) presents this correlation, where is the average clearance, C_0 and C_1 are, respectively, the inlet clearance and the outlet clearance, L is the seal length and α is the seal taper angle.

$$\left(\quad \right) \alpha \quad [(\quad) \quad] \tag{5}$$

$$\quad \tag{6}$$

$$\quad \tag{7}$$

As shown in Fig. 1, for a straight seal H is a constant number, once α is null, in other words, $H = \quad = C_0 = C_1$.

ISSN 2176-5480

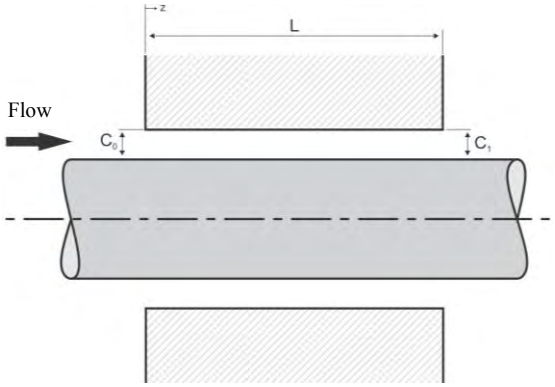

Figure 1. Straight Seal

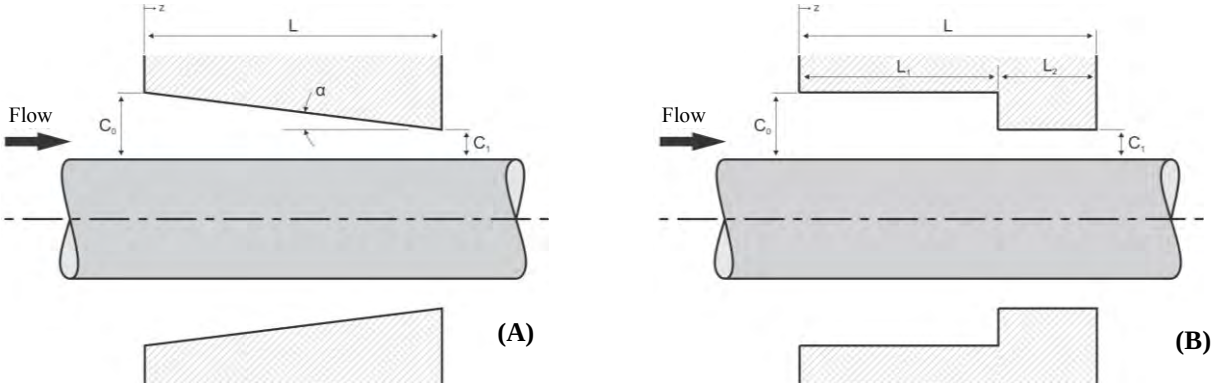

Figure 2. Other types of plain seals. (A) Tapered Seal, (B) Stepped Seal. (Adapted from Fleming (1977))

For a tapered seal, Fig. 2(A), the clearance function obey the Eq. (5), so, for each position of the seal there will be a regarding value of H. Moreover, tapered seals can be classified as divergent or convergent, this classification depends on the geometry of the seal, if C_1 is greater than C_0, then there is a divergent seal, otherwise, for a convergent seal C_0 must be greater than C_1.

The stepped seal can be analyzed as a combination of two straight seals, Fig. 2(B). Therefore, this type of plain seal has two different constant clearance functions, each one referring to the corresponding seal.

Therefore, the understanding of the straight plain seal is of fundamental importance to future steps in more complex configurations modeling.

Figure 3 shows the pressure distribution for a straight seal. At the seal inlet, there is a pressure loss due to energy dissipation caused by a shock between the fluid and the seal entrance, represented by p_s and $p(0)$. Along the seal occurs a pressure gradient, which is explained by the wall friction. This gradient is represented by a line between $p(0)$, which is the pressure in the seal entrance, and $p(1)$, which represents the pressure in the seal exit. According to Domm et al. (1967), there is a possibility of pressure recovery at the seal exit, which increases the seal's direct stiffness. This recovery is shown, in Fig. 3, as p_e.

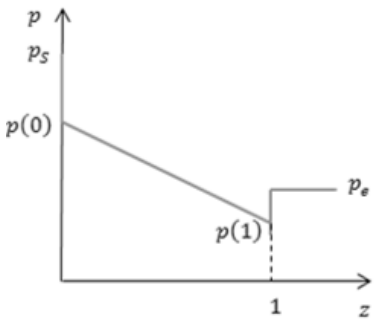

Figure 3. Pressure distribution along the seal (Brol,2011).

2.1 Finite volume method

ISSN 2176-5480

The dimensionless form of the Eq. (2), (3) and (4) is used to reduce the number of dependent variables of the system parameters, like diameter of the shaft, seal length and clearance, avoiding variations in the equations due to these parameters. Therefore the dimensionless set is properly required in order to facilitate the application of the numerical method.

$z = Z/L$ (8) $/$ (9) $/$ (10) $/$ (11)

$/$ (12) $/$ (13) $/$ (14) $/$ (15)

(16) (17) (18) (19) (20)

(21) $(\,)\ (-)$ (22) $(\,)\ (-)$ (23) (24)

Where W_0 is the average axial velocity, is the rotational speed, b represents a dimensionless parameter, F_r is the radial force and F is the circumferential force, f is the dimensionless frequency and Ω is precessional seal velocity.

In this work the finite volume is used due to limitations of an analytic solution. This numeric method allows the future analysis of complex types of seals, such as labyrinth and honeycomb seal, because its robustness regarding the fluid mechanics problems.

To solve the dimensionless form of Eq. (2), (3) and (4), the Upwind method (Maliska, 2004) was used. This method is a variation of the finite volume method and solves a problem when only the initial condition is known.

As the straight plain seal is considered centered in relation to the shaft center, the variables as pressure (P), axial (W) and circumferential (U) velocities do not change with the polar coordinate , only with z, which represents the direction of seal length. Thus, the numerical method can be particularly used only in this direction.

Figure 4 represents the finite volume method applied for the pressure, i is the numerical variation due to z. For Upwind method, p_{i+1} is similar to p, once its value is unknown.

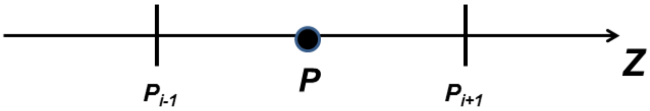

Figure 4. Representation of the volume P in the numerical mesh.

2.2 Determination of dynamic coefficients

After solving continuity, axial-momentum and circumferential-momentum equations for centered seal and for a small motion about a centered position, it is possible to determine the reaction-forces through the numerical integration of the pressure distribution along the seal.

Besides, Eq. (1) is modified from rectangular to polar coordinate system, and using a frequency-response solution despite of the displacement, velocity and acceleration of the shaft.

Equation (25) represents the dimensionless dynamic coefficients in terms of reaction-force components, (radial, f_r,and circumferential, f_θ).

$$(\,)\ (\,)\quad (25)$$

The dynamic coefficients are obtained by calculating the reaction-forces for a range of dimensionless frequency values, from null to two, and then, through Eq. (25), the coefficients are determined using a least squares curve fit.

3. RESULTS

The dynamic coefficients, determined by a nominal straight seal, is defined by the parameters presented in Tab. 1

ISSN 2176-5480

Table 1. Parameters of the analyzed straight seal.

Pressure gradient (ΔP)	35 bars = 35E05 Pa
Seal length (L)	0.0508 m
Radius of the shaft (R)	0.0762 m
Inlet and outlet clearance (C_0 and C_1)	3.81E-04 m
Rotational speed (ω)	3000 rpm = 314.2 rad/s
Density (ρ)	1000 kg/m^3
Absolute viscosity (μ)	1.3E-03 kg/m.s
Relative stator and rotor roughness (ϵ_s and ϵ_r)	0.001
Inlet-loss coefficient (ξ)	0.10
Exit-recovery coefficient (ξ_e)	1.0

The result of this analysis is shown at Tab. 2 with comparative values in the literature (Childs, 1993).

Table 2. Calculated values for straight seals dynamic coefficients.

	K_x10^{-7} [N/m]	k_x10^{-6} [N/m]	C_x10^{-5} [N.s/m]	c_x10^{-4} [N.s/m]	M [kg]
Calculated	1.567	0.473	0.301	0.210	6.68
Childs (1993)	1.567	0.473	0.300	0.210	6.68

It is possible to verify, from Tab. 2, that the solution method for dynamic analysis accomplished in this work presents satisfactory values of dynamic coefficients in relation to the data presented by Childs (1993). Besides, it is also important to note that in Childs (1993) an analytical analysis was employed.

Beyond the results presented in Tab. 2, the influence of several physical and operational parameters for a nominal plain seal is verified. These parameters are: L/D, where D is the diameter of the shaft; $\bar{\ }$ /R; ξ; ξ_e; ϵ_s; ΔP and ω, which are, respectively, ratio between seal length and shaft diameter; ratio between the clearance and shaft radius; inlet loss coefficient; exit recovery coefficient; stator relative roughness; pressure gradient and rotational speed.

Figure 5 represents the variation of L/D and the response of the dynamic coefficients.

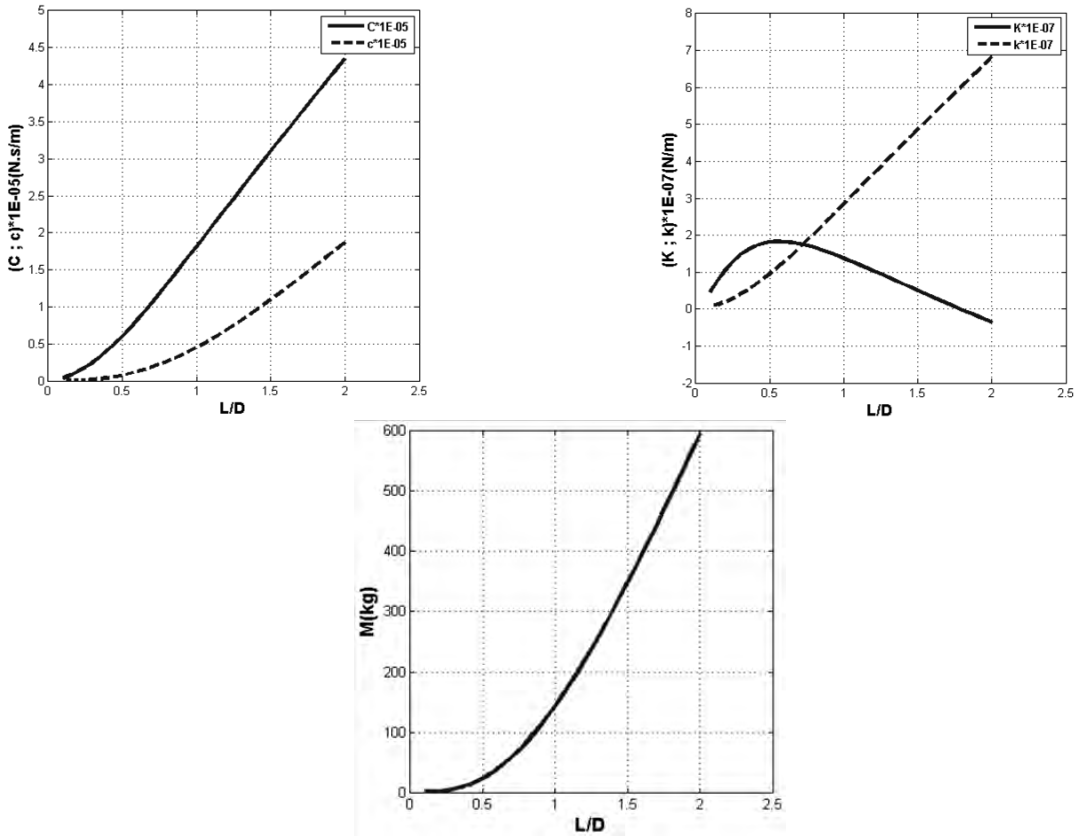

Figure 5. Dynamic coefficients versus L/D.

ISSN 2176-5480

Figure 5 shows that damping (direct and cross-coupled), cross-coupled stiffness and inertia coefficients increase with increasing L/D. However the direct stiffness coefficient has a maximum around L/D = 0.5 and then decreases, becoming negative from L/D = 1.75. This happens because increasing the ratio L/D, decreases the influence of inlet loss on pressure distribution, thereby the "Lomakin effect" reduces and, as consequence, the direct stiffness. Another effect is the increase of inertia term, which assumes a very high value for long seals.

Figure 6 represents the dynamic coefficients in function of the variation of $\bar{}$ /R. For this analysis, the ratio L/D was maintained at 0.5, in other words, L = R = 0.0762 m.

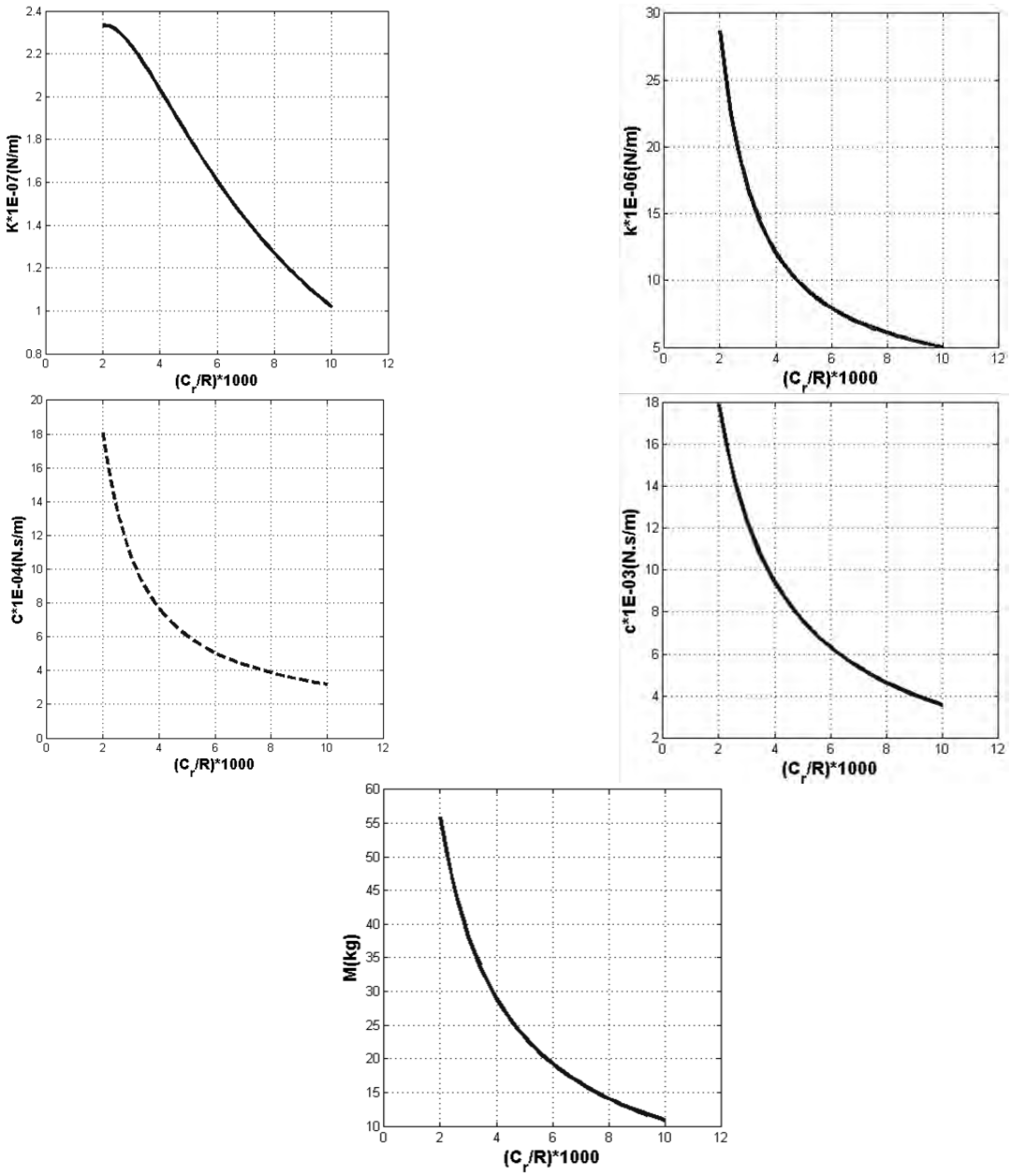

Figure 6. Dynamic coefficients versus $\bar{}$ /R, with L/D = 0.5.

All coefficients, in Fig. 6, decrease with the increasing of the $\bar{}$ /R ratio. Particular importance must be given for direct stiffness and damping terms. According to Childs (1993), the reduction of direct stiffness can commonly cause a shift of the critical speed into the operating rotational speed range. Besides, the loss of direct damping means much sharper response of the rotor motion.

Figure 7 illustrates the influence of inlet loss coefficient on the dynamic coefficients.

ISSN 2176-5480

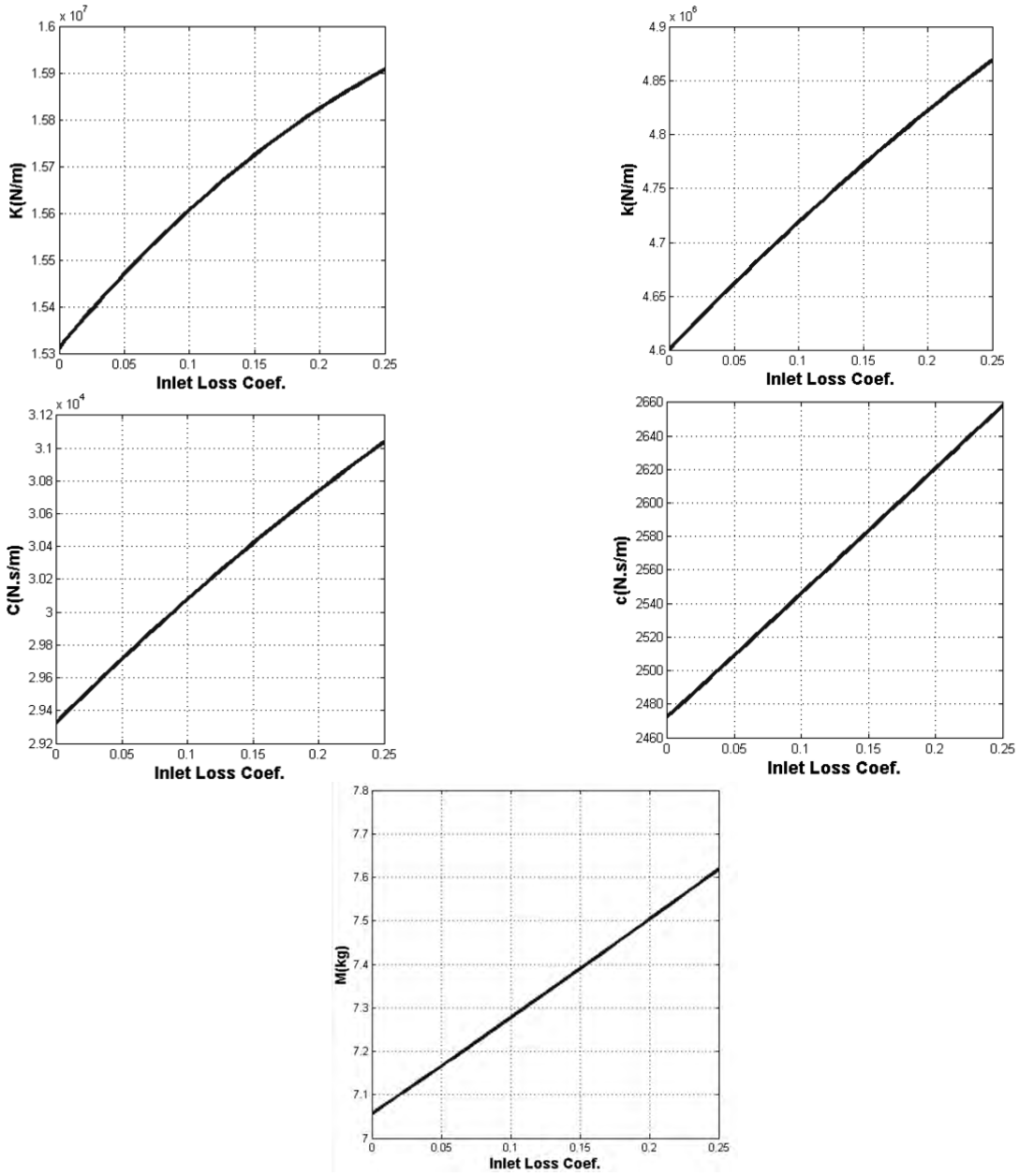

Figure 7. Dynamic coefficients versus ξ. (¯ /R = 0.005 and L = 0.0508 m)

As expected, the coefficients increase with the rise of the inlet loss parameter, since the influence of inlet loss pressure increases the pressure gradient. However, changing ξ from 0 to 0.25, the direct stiffness only change about 4%, despite the strong dependence on "Lomakin effect". The other dynamic coefficients also present a small percent of variation, for k, C, c and M these variations are, respectively, 6%, 6%, 8% and 8%.

Figure 8 shows the response of the dynamic coefficients with respect to the exit recovery coefficient variation. In this analysis, the ratio L/D was maintained at 0.5, ξ is 0.10 and ¯ /R at 0.005.

ISSN 2176-5480

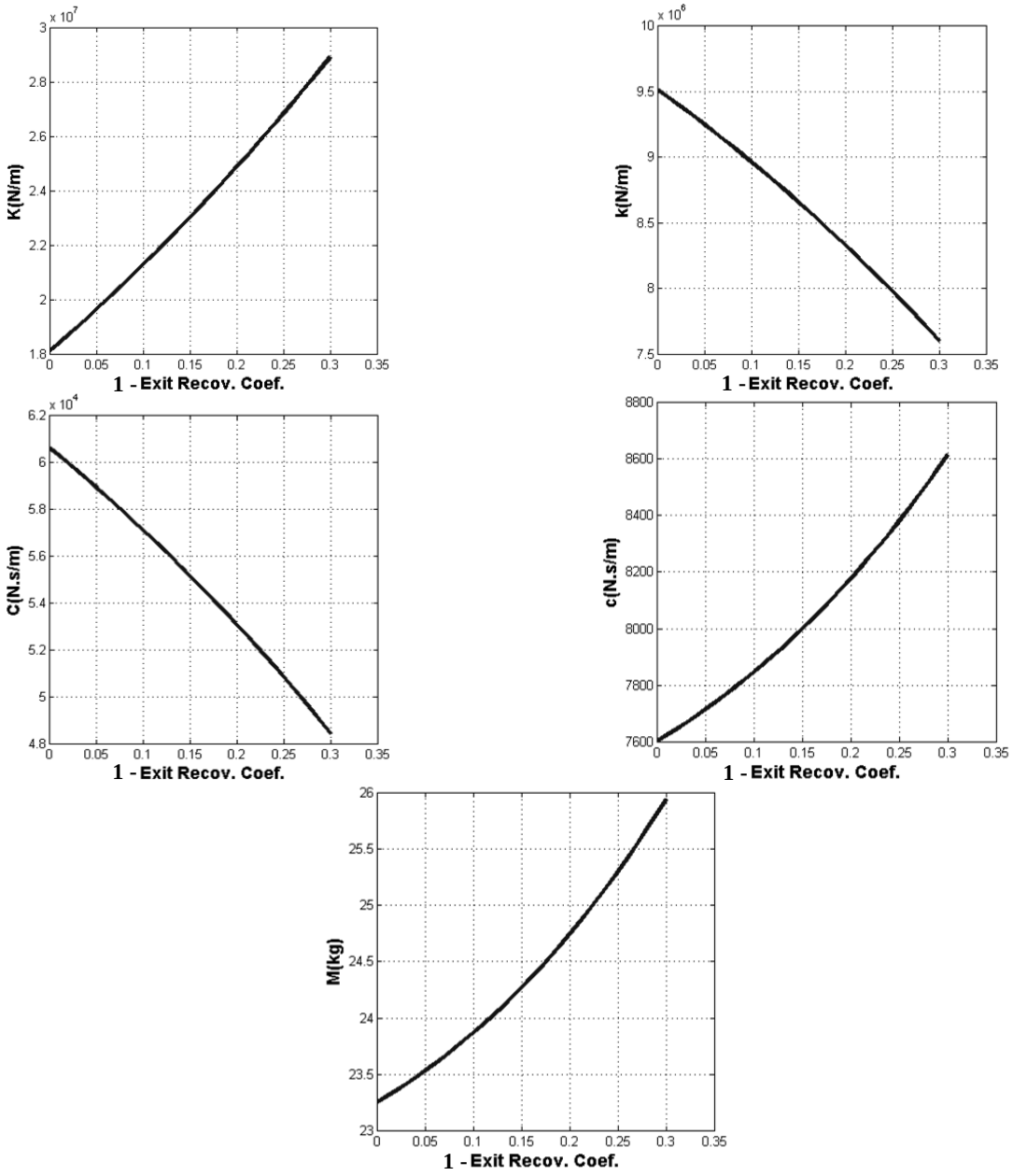

Figure 8. Dynamic coefficients versus (1-ξ_e), with L/D = 0.5, $\bar{}$ /R = 0.005 and ξ = 0.10 .

For ξ_e = 1, in other words (1 - ξ_e) = 0, there is no pressure recovery on the exit of the seal. As reported by Domm et al (1967), the more the effect of pressure recovery occurs, the more direct stiffness raises. In fact, this is the dynamic term with the largest influence of $\xi_{e,}$, (about 60% of variation).

Figure 9 illustrates the variation of stator relative roughness and the response of the dynamic coefficients. In this case, the ratio L/D was equal to one, meaning L = 0.1524 m and the other parameters are maintained as in Tab. 1.

ISSN 2176-5480

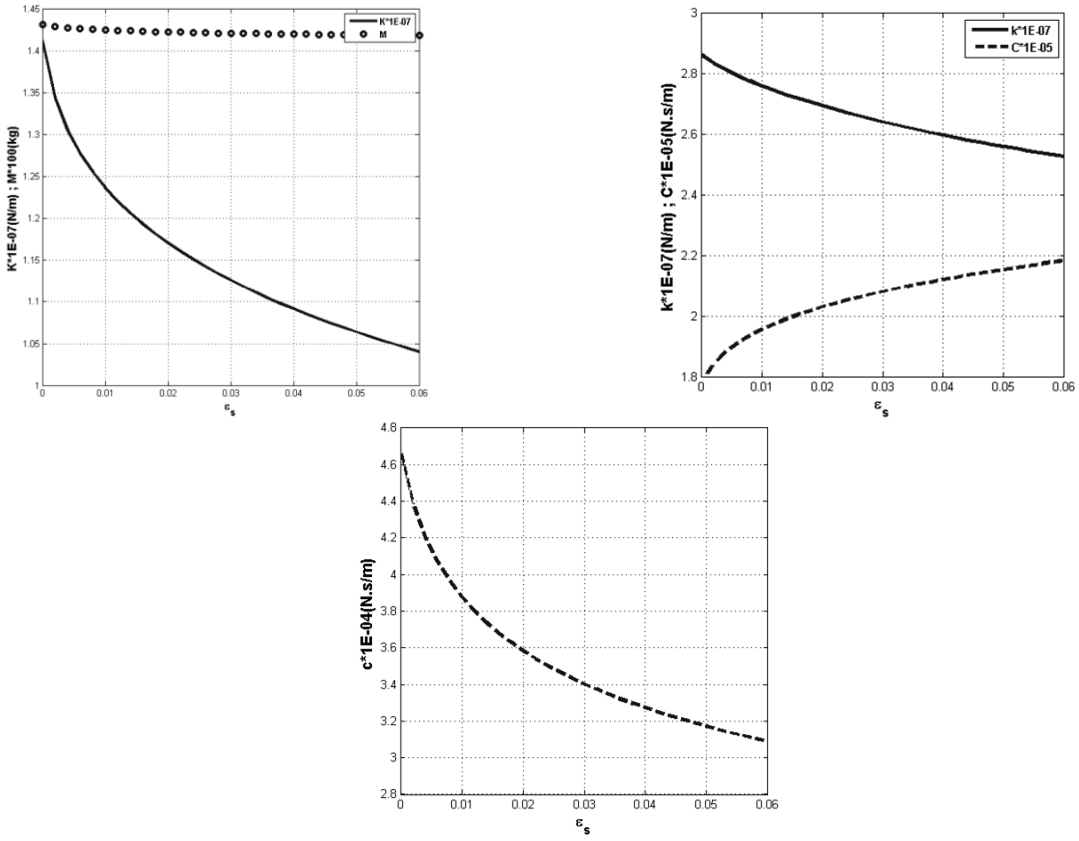

Figure 9. Dynamic coefficients versus ϵ_s.

The behavior of the direct stiffness term, in Fig. 9, is associated not only with change in ϵ_s, but it is also related with Fig. 5. Because increasing ϵ_s and L/D, as explained before, the portion of pressure loss on the seal entrance decreases, which reduces the "Lomakin effect" and, consequently, K. However, the inertia coefficient is practically insensitive to change in ϵ_s in spite of changes in L/D.

Figure 10 represents the cross-coupled and direct stiffness and direct damping terms as a function of pressure gradient (ΔP).

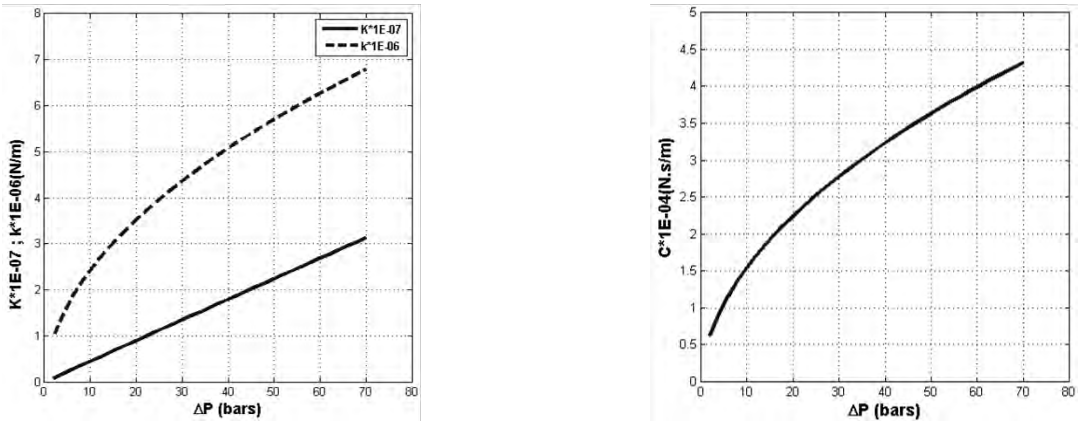

Figure 10. Dynamic coefficients versus ΔP.

The cross-coupled damping and inertia terms are not presented in Fig. 10 because they are insensitive to changes in pressure gradient. Apart these coefficients, direct stiffness increases linearly with ΔP, besides cross-coupled stiffness and direct damping also increase, but not as a linear function.

Figure 11 shows the dependence of the dynamic coefficients on the rotation speed. It is important to notice that pressure gradient is also a quadratic function of ω. Then, for each value of ω there is also a new value for ΔP.

ISSN 2176-5480

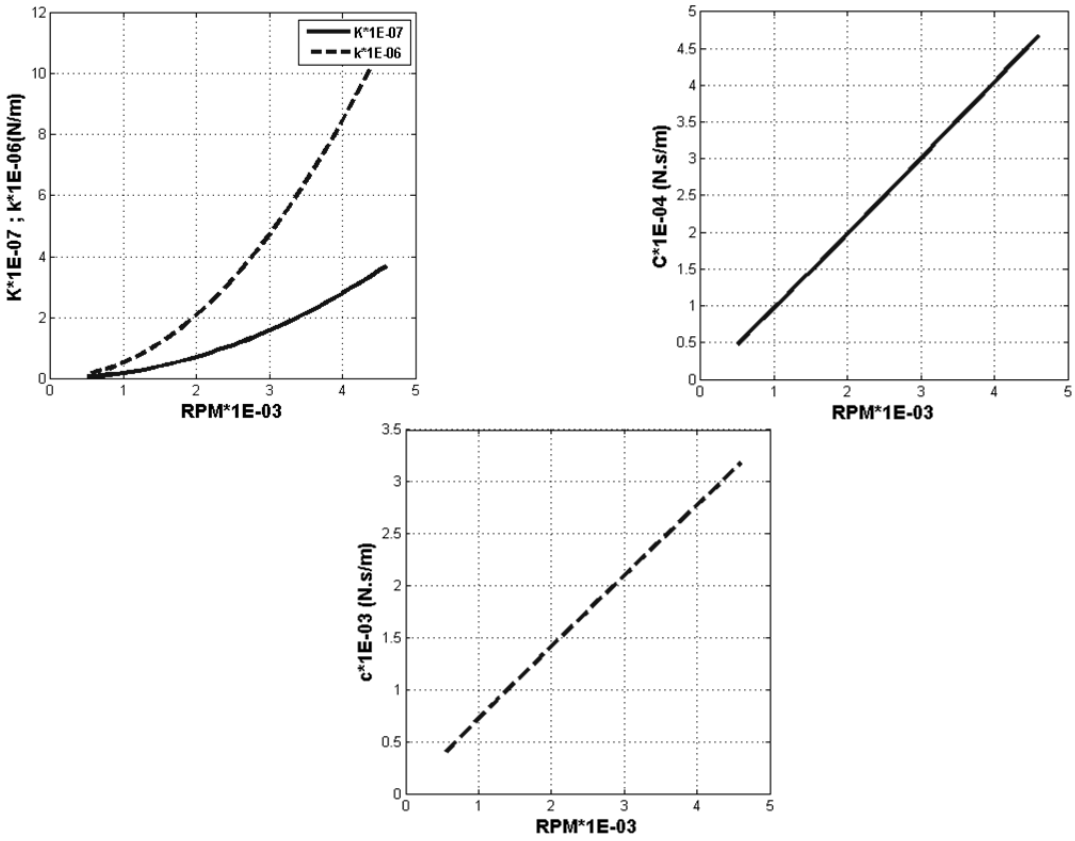

Figure 11. Dynamic coefficients versus ω.

Once again the inertia coefficient do not change with variation of ω, and because of that, it is not represented in Fig. 11. Damping terms are a linear function of rotational speed while stiffness terms changes as a quadratic function of ω. All the parametric analysis is in agreement with the literature (Childs, 1993).

4. CONCLUSIONS

Fluid seals present a turbulent behavior due to the large clearance between shaft and seal, high pressure drop across the seal and high axial velocity. Because of that, this component cannot be analyzed through Reynolds' equation. Thus the continuity, axial-momentum and circumferential-momentum equations must be used to examine mechanical seals.

The data obtained for dynamic coefficients of a nominal straight seal is consistent with the specialized literature (Chlids, 1993). Therefore, the numerical method used, i.e. finite volume method, produces a satisfactory outcome on the analysis of fluid seal. This is important for future studies of seals with more complex geometries.

Finnaly, it was possible to conclude that the dynamic coefficients, and so the straight seal, depend on many physical and operational parameters, such as the rotational speed (ω), pressure gradient (ΔP), stator relative roughness (ϵ_s), ratio between seal length and shaft diameter (L/D), inlet loss coefficient (ξ), exit recovery coefficient (ξ_e) and ratio between clearance and radius of the shaft (¯ /R).

Particularly, it is important to point out that stability condition can be strongly affected by these parameters, due to its dependence on stiffness cross-coupled and direct damping coefficients.

5. ACKNOWLEDGEMENTS

The authors thank CNPq and FAPESP for the financial support on this research.

6. REFERENCES

Brol, K. B. *Modelagem e Análise de Selos de Fluxo Aplicados a Máquinas Rotativas*, Dissertação (Mestrado em Engenharia Mecânica) - Universidade Estadual de Campinas, Campinas, 2011.

Childs, D. W. *Turbomachinery Rotordynamics: Phenomena, Modeling, and Anaysis*; John Wiley & Sons, New York, 1993.

ISSN 2176-5480

Domm, V.; Dernedde, R., Handwerkwe, TH. Der Einfluss der Stufenabdicktung auf die Kritische Drezahl von Kessel Speisepumpen. *VDI-Berichte*, n.113, 25-28 p, 1967.

Fleming, D. P. High Stiffness Seals for Rotor Critical Speed Control. *Technical paper to be presented at the Vibrations Conference sponsored by the American Society of Mechanical Engineers*, Chicago, Illinois, September 26-29, 1977

Fox, R. W.; Mcdonald, A. T.; Pritchard, P. J. *Introdução à mecânica dos fluidos*; LTC, 6ª edição, 2006.

Kwanka, K. Dynamic coefficients of stepped labyrinth gas seals. *Journal of Engineering for Gas Turbines and Power*, v. 122, pp. 473-477, July 2000.

Lomakin, A. A. Calculation of critical speeds and securing of the dynamic stability of hydraulic high-pressure machines with reference of the forces arising in the gap seals. *Energomashinostroenie*, 4.1, 1958

Maliska, C. R., *Transferência de Calor e Mecânica dos Fluidos Computacional*; Editora LTC, 2º edição, Rio de Janeiro, Brasil, 2004.

Reynolds, O., On the Theory of Lubrication and Its Application to Mr. Beauchamp Tower's Experiments Including an Experimental Determination of the Viscosity of Olive Oil. *Philos. Trans. R. Soc. London*, Series A, Vol. 177, Part 1, 1886, pp.157-234.

Shen, X.Y.; Jia, J. H.; Zhao, M.; Jing, J. P. Numerical and experimental analysis of the rotor-bearing-seal system. *Journal of Mechanical Engineering Science* v. 222, part C, pp. 1435-1441, 2008.

Vance, J. M. *Rotordynamics of Turbomachinery*; John Wiley & Sons, New York, 1988.

7. RESPONSIBILITY NOTICE

The authors are the only responsible for the printed material included in this paper.